Experimental characterization and numerical modeling of the compressive mechanical behavior of hazelnut kernels

Published version:

DOI:10.1016/j.jfoodeng.2015.06.037

Experimental characterization and numerical modeling of the compressive mechanical behavior of hazelnut kernels

Cristiana Delprete[1], Simone Giacosa[2], Emanuele Raviolo[1],
Luca Rolle[2], Raffaella Sesana[1*]

[1]Politecnico di Torino, Department of Mechanical and Aerospace Engineering (DIMEAS), Corso Duca degli Abruzzi 24, 10129 Torino, Italy.
[2] Università di Torino, Dipartimento di Scienze Agrarie, Forestali e Alimentari (DISAFA), Largo Paolo Braccini 2, 10095 Grugliasco (TO), Italy.

Abstract

The evaluation of mechanical properties of hazelnuts has been developed over the past years mainly to optimize industrial processes. The aim of this study is to reproduce the compressive behavior of hazelnut kernel obtained by experimental and numerical activities; the contribution of pellicle influence to the mechanical behavior is also analyzed.
The experimental activity is aimed to measure the mechanical properties of hazelnut kernel and to obtain a model calibration based on experimental data analysed by statistical approach. The finite element models of hazelnut kernels are implemented and a set of numerical compression tests are simulated; the comparison of experimental and numerical responses is shown.

Keywords: Hazelnut kernel, mechanical properties, finite element model

1. Introduction

The hazelnut *Corylus avellana L.* is native of an area that stretches from Europe to south west Asia and has been introduced in USA (California State) and several other countries around the world. Turkey is the largest producer of hazelnuts in the world with approximately 75% of worldwide production, followed by Italy, USA and Spain (FAO, 2014).

The nut kernel is the edible part of the hazelnut. Many studies have been conducted regarding its internal structure, some of them dating back to the first years of the XX century (Winton, 1906; Young, 1912). The edible kernel is covered by a removable thin fibrous pellicle, with the internal tissue of the cotyledons consisting of parenchyma cells separated by very small intercellular spaces (Young, 1912).

The hazelnut kernel is widely used in the food industry as fruit, grounds and in form of flour. The roasting process is used to achieve an optimal flavor development and intensity of taste, as for it modifies the physical, chemical and sensory characteristics.

The evaluation of mechanical properties of hazelnuts (whole fruit, shell, kernel) has been developed over the past years with the objectives to obtain industrial processes and improve the use of hazelnuts as food ingredient. The easiness to break and to remove the nut shell was evaluated on Turkish varieties (Güner et al., 2003; Ozdemir and Akinci, 2004; Ercisli et al., 2011) and also on nut varieties intended for fresh table consumption (Valentini et al., 2006). Nut shell characteristics, such as hardness and thickness, were measured and correlated to the biological cycle of the nut weevil of *Curculio nucum* (*Coleoptera: Curculionidae*) pest and to the damage by its larvae (Guidone et al., 2007) stress the importance of physical properties evaluation.

The physical characteristics of the hazelnut kernel have an important role on the crispness and crunchiness sensory parameters especially on the roasted nuts (Saklar et al., 1999) and the water activities have direct effects on mechanical characteristic (Borges and Peleg, 1997). The overall quality is influenced by oxygen and relative humidity contents during the product storage (Ghirardello et al., 2013). Di Matteo et al. (2012) evaluated also some mechanical properties of chemical-peeled hazelnut kernels, such as firmness and rigidity, to study an original industrial process to improve the kernel pellicle removal. A mechanical characterization of whole nut, kernel and shell was conducted (Delprete and Sesana, 2014) in order to aid the design and construction of selecting machines.

The main aim of this study is to obtain, by experimental and numerical activities, the model of the compressive behavior of hazelnut kernel and to investigate the role of the pellicle coating and roasting process; the here investigated variety of hazelnut is the *Tonda Gentile Trilobata*.

The present study measures the mechanical properties of the kernel material, raw and roasted, selects and calibrates the proper constitutive material model for numerical simulations, and investigates the behavior of the whole hazelnuts in the same experimental conditions (raw and roasted). Finally the research identifies the average value of the investigated mechanical parameters, the variability of the measurements and the influence of the number of the specimens within a single sample. The implementation and validation of a numerical finite element (FE) model of hazelnut based on geometric and material data is reported.

2. Materials and methods

Experiments were carried out to obtain the empirical data of material behavior.

The geometry of real kernel has been computed by means of TAC scanning of four kernels and this has been used to define ~~a~~ numerical modeling. Material calibration data has been derived from experimental test activity on specimens obtained from the same four kernels.

2.1. Experimental tests

The hazelnut sample was composed of about 5 kg of conform and raw *Tonda Gentile Trilobata* (formerly known as *Tonda Gentile delle Langhe*) Italian autochthonous cultivar (2013 harvest).

The moisture content, determined according to the AOAC 925.40 method (AOAC, 2000), was of 4.45% ± 0.57% w.b.

Geometric parameters and mass of kernels were acquired as described in a previous work (Delprete and Sesana, 2014).

According to χ^2 test and normal distribution test, the samples distributions were checked to be normal. By means of Chauvenet test (Montgomery et al., 2001) measurements anomalies were excluded from data processing. Minimum sample size was identified by means of plotting percent relative deviation vs specimen number, selecting the sample size corresponding to percent relative deviation settling to a steady value.

For roasting process, about 2 kg hazelnuts were put in oven ~~roasted~~ at 140 °C of ~~roasting~~ temperature during 30 minutes (Donno et al., 2013). Moisture content of roasted hazelnuts, at the time of analysis, was 2.40%±0.31% w.b.

Compressive tests were performed based on the previous studies (Delprete and Sesana, 2014; Valentini et al., 2006; Ghirardello et al., 2013).

In particular, a reference system has been defined on the kernel indicating three main directions and dimensions as reported in Figure 1. The testing machine is a TA.XTplus texture analyzer (Stable Micro Sytems, Godalming, UK), with loading speed 6 mm/min (down plate moving). For all tests, the average curve was calculated by Matlab R2010b software, by means of dedicated routines developed for the present research activity. Each considered sample ~~is composed~~ consisted of at least 50 specimens.

To optimize the experimental conditions that allow the best monitoring of the measurement changes, (according to Torchio, et al., 2012), and to evaluate the influence of the sample size on the variability in the measurements, the optimum sample size was assessed representing the relative standard deviation (RSD) values against the number of measurements for each parameter. The stabilization of the RSD assessed the minimum sample size.

The first test sample (Sample 1) is composed of 50 just shelled raw hazelnut kernels while the second (Sample 2) is composed of 50 manual peeled raw hazelnut kernels; that is, in the former case the kernels are provided with pellicle while, in the latter one, the pellicle has been removed by a careful hand scraping procedure. In particular, by means of a sharp razor and a lens, the pellicle has been carefully removed, taking care of not cutting away kernel material. In both cases the kernels are compressed along the *A* direction (Delprete and Sesana, 2014). In Figure 2 the test setup is presented.

Figure 1: Hazelnut shell and kernel main dimensions.

Figure 2: Kernel compression along *A* axis, experimental setup.

The third test sample (Sample 3) is composed of 50 roasted hazelnut kernels; pellicle was removed, as the roasting procedure makes it to detach from the kernels. As in the previous cases, the testing procedure consists in a compression along the *A* direction.

From these three sets of tests, the force-displacement curves were acquired, the average maximum load ($\bar{L}_{kf}$) to break the hazelnuts and the slope (stiffness $\bar{K}$) of the linear part of the compression curve were calculated for each specimen within the corresponding sample. It has to be noted that the hazelnut failure force was defined as the force needed for the separation of the two cotyledons (Figure 3). For each of these parameters, χ^2 test was done to verify the normality of distributions and the relative standard deviation analysis was done to optimize the sample size.

Figure 3: Compression failure of hazelnut kernel: cotyledon separation.

The fourth (Sample 4) and fifth (Sample 5) test samples are composed of raw and roasted kernel specimens, respectively (Figure 4 a), undergoing compression test (Figure 4b). The specimens are cylindrical, 5 mm high and 5 mm diameter, and they are obtained by means of two dedicated tools: the first tool cuts a slice (thickness of 5 mm) from the kernel with two parallel surfaces, the second tool is a circular blade of 5 mm diameter and it cuts a cylinder from the kernel slice. Cylinders were cut without taking into account of the direction as the kernel material results to by hysotropic (Delprete and Sesana, 2014). The kernel specimens were obtained from each of the four described groups of hazelnuts, ~~basing~~ based on their kernel conformity.

Figure 4: Kernel specimens a) and specimens compression setup b).

From these two sets, the stress-strain curves were acquired, the average maximum stress to break the specimens (UCS), the slope (elastic modulus $\bar{E}_k$) of the linear part of the curves and the knee stresses (σ_k) were calculated (Delprete and Sesana, 2014).

The sixth experimental sample was concerned about four raw kernels without pellicle. By using computed tomography analysis (CTA) these four raw kernels were scanned and the actual geometry including the inner cava was digitalized. The four raw kernels were compressed until cotyledon separation and, from the cotyledons of each of them, cylindrical kernel specimens were obtained and compressed. Results obtained were processed to obtain the above-mentioned parameters, but without average calculation. ~~hen,~~ These results have been compared with the results of previous samples to check if they could belong to the same range of results.

The corresponding constitutive curves were used to calibrate the numerical FE models of each kernel. Finally the simulation of compression of the kernel was run.

2.2. Numerical modeling

The numerical analysis was carried out with the commercial finite element software ABAQUS 6.11-1.

Compression tests showed that the hazelnut kernel is elastic and isotropic and then the material constitutive model selected for the FE model is elastic isotropic. To calibrate the model, the elastic modulus was measured following the procedure described in (Delprete and Sesana, 2014). The Poisson's ratio was not measured and, as a first approximation, it was kept constant to 0.3.

Geometry information was acquired by CTA; the output STL file discretizes the outer surface and the internal cavity surface with 0.4 mm resolution. Due to the extremely large number of elements, a re-mesh operation was carried out; moreover the space between the inner and the outer surface was filled by 4-node linear tetrahedron elements. Table 1 gives a comparison of the number of nodes and elements for each hazelnut kernel.

Table 1: Elements and nodes of numerical hazelnuts.

The simulation aims to reproduce the experimental tests, in which the hazelnuts are compressed between two steel plates. Two infinite stiff plates simulate these plates because the elastic modulus of steel is four orders of magnitude greater than that of the hazelnuts; this choice guarantees a lower computational time.

A zero displacement boundary condition is imposed on the lower plate and a 2 mm boundary condition on the upper plate.

Some nodes in the lower part of the hazelnut mesh were constrained to the lower plate by low stiffness spring elements to ensure solution convergence. Volume force corresponding to gravity effect is imposed on the whole model.

The analysis type is static and the numerical implicit procedure is based on Newton-Raphson method, which allows obtaining solutions for non-linear problems. In this case the source of nonlinearity is not represented by the material but by the geometry, whose changes during the simulation are not negligible.

The contact formulation is based on a surface-to-surface discretization, so contact conditions are enforced over regions around slave nodes rather than only at individual nodes (ABAQUS Analysis User's Manual). The plates are the master surfaces while the hazelnut is the slave surface.

The contact property between the plates and the hazelnut is assumed as Coulomb friction model with constant coefficient $\mu = 0.3$.

3. Results and discussion

3.1. Experimental testing

3.1.1. Physical properties

The mass measurement distribution of hazelnut kernels can be assumed as a normal distribution (positive χ^2 test, 85% confidence level); the corresponding average and standard deviation values and the sample size are reported in Table 2.

For what concerns geometric measurements, statistical analysis was run on A/B, C/B and C/A values (Delprete and Sesana, 2014). The distribution of these ratios can be assumed as a normal distribution (positive χ^2 test, 85% confidence level) with average values and standard deviations reported in Table 2.

The obtained mass and geometric results show a distribution which is coherent with analogous results described in (Delprete and Sesana, 2014).

Table 2: Average values and standard deviations of physical and geometrical measurements on the specimen samples.

3.1.2. Whole kernel mechanical properties

In Figure 5 experimental force-displacement curves of raw kernels with and without pellicle (Sample 1 and 2 respectively) are reported along with the average calculated curves.

Stiffness distribution of raw kernels with pellicle can be assumed as a normal distribution and the corresponding values are reported in Table 3; also the load to failure distribution gives a positive χ^2 test and so can be considered normal. For both these parameters it is possible to define a minimum sample size by means of the stabilization of the percent relative standard deviation. The 70% of the sample presents a defined failure point; for the remaining specimens the corresponding point is not recognizable on the curves.

Figure 5: Force-displacement raw kernel curves with (blue) and without (red) pellicle. Average curves are respectively the green and the cyan ones.

For what concerns Samples 2 and 3, that is raw and roasted kernels without pellicle, both stiffness and load to failure are normally distributed; the mean and standard deviation values are reported in Table 3. The 64% of the Sample 2 and the 58% of the Sample 3 present a defined failure point. In both cases it is possible to define a minimum sample size both for the stiffness and for the load to failure because of the stabilization of the percent relative standard deviation.

In Figure 6 experimental force-displacement curves of roasted kernels are reported along with the average calculated curve.

Figure 6: Force-displacement roasted kernel curves with average curve (white).

The normality of the stiffness distributions leads to the definition of a 95% confidence level interval. In Figure 7 three intervals are shown, corresponding to raw kernels (with and without pellicle) and roasted kernels. The two raw kernel intervals have an intersection but a consistent part of the raw with pellicle interval extends above the raw without pellicle one. On the other side the lower part of the raw without pellicle interval lies below the raw with pellicle one. So the presence of the pellicle has an important effect on the compressive behavior of the kernel; in particular, as it is shown in Figure 5, it increases the average stiffness.

Figure 7: Raw kernels with (blue continuous lines) and without (red continuous lines) pellicle and roasted without (black continuous lines) pellicle: 95% stiffness values limits.

The roasted kernel interval is just a little greater than the raw with-pellicle interval and so the corresponding average curves are very similar. This means that the material properties have increased due to baking; in particular the roasted kernels have obtained almost the same average stiffness as the raw with pellicle kernels.

These results show a distribution which is coherent with analogous results described in (Delprete and Sesana, 2014). The numerical values varied ~~are therefore different~~ as a different moisture level is present in the examined sample and it is well known (Koyuncu et al., 2004; Guner et al., 2003) that for wood and shells this property influences the mechanical properties.

Table 3: Mechanical properties measurements on the whole kernel samples.

3.1.3. Kernel specimens mechanical properties

For the two Samples 4 and 5 the stiffness distributions can be considered normal. The average value, the standard deviation and the minimum sample size are shown in Table 4.

Table 4: Mechanical properties measurements on the kernel specimen samples.

Experimental stress-strain curves can show, in the range 0-1.5 mm displacement, two distinctive trends; the first consists in a clear change of slope of the curve, the second in the presence of a maximum. As regards raw kernels, the 34% of the sample shows a change of slope, the 51% a maximum and a 15% neither of them. On the other hand the 70% of roasted kernels shows a change of slope, the 18% a maximum and the 12% neither of them.

These results show a distribution, which is coherent with analogous results described in (Delprete and Sesana, 2014). As stated above, the numerical values are therefore different as a different moisture level is present in the examined sample and it is well known (Koyuncu et al., 2004; Guner et al., 2003) that for wood and shells this property influences the mechanical properties.

3.1.4. CTA scans

The digital geometry of Sample 6 specimens was obtained by means of General Electric Phoenix V|tome|x m, a versatile X-ray micro-focus computed tomography system for 3D metrology and analysis. It allows carrying out non-destructive testing tasks with less than 1 μm detail detectability. As stated above, the outer and the inner surfaces of the hazelnut kernels were discretized with 0.4 mm resolution by the measurement system and then a re-mesh process has led to a strong reduction of elements. In Figure 8 the external a) and internal c) surfaces, supplied by computed tomography, and the same surfaces after the re-meshing process b) and d) are reported as an example.

Figure 8: External a) and internal c) surfaces by CTA and after re-meshing elaboration b) and d).

3.2. Numerical simulations

As shown in Table 4, the elastic modulus values are distributed as a normal both for raw kernels and roasted kernels, so it is possible to define a 95% level confidence interval for both samples. In particular, as regards raw kernels, the lower and the upper limit are, respectively 6.4 MPa and 16.9 MPa. For each hazelnut kernel three simulations have been carried out, that is three different values of elastic modulus have been considered: the lower limit, the mean and the upper limit. In Figure 9 the simulation results are plotted along with the 95% limit curves of Sample 2.

Figure 9: Comparison between numerical results (black, red and green lines) and 95% limit curves (blue lines).

The black, red and green curves are obtained, respectively, with the lower limit, the mean and the upper limit stiffness values. The comparison of the curves outlines the influence of the geometry of the kernel: for example the upper limit curve in case b) assumes lower values with respect to case c). Moreover also the area delimited by the upper and lower limit curves is very different from case b) to case c).

The upper limit curve (green curve) lies, in all cases, between the 95% limit curves (blue curves) so it gives a good approximation of the compressive behavior of the hazelnut kernel;

the mean curve (red curve) is almost coincident with the lower limit curve and the lower limit curve (black curve) lies out of the 95% range. So the stiffness values that better describe the compressive behavior of the hazelnut are included in the upper part of the Gaussian distribution.

4. Conclusions

A procedure to define a numerical model of kernel compression testing has been described. The geometric model has been defined by means of 3 dimensional scanning of actual hazelnuts. The constitutive material model has been selected according to experimental evidence as linear elastic. The calibration parameters were obtained by means of processing experimental data.

Experimental data acquisition and processing took a relevant time lapse as it allowed defining many points as the sample size, the best experimental data fitting curve and corresponding confidence interval, the simulation results reliability.

Experimental testing also pointed out that the compression of with and without pellicle kernels outlined the influence of pellicle on mechanical behavior, that is, an increase of the overall stiffness of the kernel. The affecting effect of moisture on compression mechanical properties was confirmed.

The results show the influence of the geometry on the compressive behavior and outline an underestimation of the elastic modulus; the underestimation is because the upper values of the Gaussian distribution allow the numerical curves to lie between the 95% limit experimental curves. This can be attributed to the approximation induced by the choice of a perfect elastic material and to the great practical difficulty in extracting cylindrical kernel specimen. A good approximation has been however achieved.

Acknowledgments

The research work was sponsored by PIEDMONT REGION within the ITACA Project (Lines POR-FESR Axis 1: Innovation and production transition, Measure I.1.1: Innovative platforms and POR-FEASR Axis 1: Improving the competitiveness of agriculture and forestry, Measure 124: Cooperation for development of new products, processes and technologies in agriculture, food and forest sectors).

We gratefully thank Dr. Scatà and laboratory technicians of LABORMET DUE srl (Torino) for precious help and counseling with CTA scanning.

References

ABAQUS 6.11-1. (2011). Analysis User's Manual.

AOAC (2000), Official Methods of Analysis, 17th Edn, no 925.40, Association of Official Analytical Chemists, Washington, DC, USA.

Borges, A., Peleg, M. (1997). Effect of water activity on the mechanical properties of selected legumes and nuts. *Journal of the Science of Food and Agriculture*, 75, 463-471.

Delprete C., Sesana, R. (2014). Mechanical characterization of kernel and shell of hazelnuts: Proposal of an experimental procedure. *Journal of Food Engineering*, 124, 28–34.

Di Matteo, M., Albanese, D., Liguori, L. (2012). Alternative Method for Hazelnuts Peeling. *Food and Bioprocess Technology*, 5, 1416-1421.

Donno, D., Beccaro, G.L., Mellano, G.M., Di Prima, S., Cavicchioli, M., Cerutti, A.K., Bononous, G. (2013). Setting a protocol for hazelnut roasting using sensory and colorimetric analysis: influence of the roasting temperature on the quality of Tonda Gentile delle Langhe cv. Hazelnut. *Czech Journal of Food Sciences*, 31(4), 390-400.

Ercisli, S., Ozturk, I., Kara, M., Kalkan, F., Seker, H., Duyar, O., Erturk, Y. (2011). Physical properties of hazelnuts. *International Agrophysics*, 25, 115-121.

FAO (2014) FAOSTAT. 2012 data. Food and Agriculture Organization of the United Nations, Rome, IT.

Ghirardello, D., Contessa, C., Valentini, N., Zeppa, G., Rolle, L., Gerbi, V., Botta R. (2013). Effect of storage conditions on chemical and physical characteristics of hazelnut (Corylus avellana L.). *Postharvest Biology and Technology*, 81, 37-43.

Guidone, L., Valentini, N., Rolle, L., Me. G., Tavella, L. (2007). Early nut development as a resistance factor to the attacks of Curculio nucum (Coleoptera: Curculionidae). *Annals of Applied Biology*, 150, 323-329.

Güner, M., Dursun, E., Dursun, İ.G. (2003). Mechanical behavior of hazelnut under compression loading. *Biosystems Engineering*, 85, 485–491.

Koyuncu, M.A., Ekinci, K., Savran, E. (2004). Craquing characteristics of walnut. *Biosystems Engineering*, 87, 305–311.

Montgomery, M. C., Peck, E. A., Vining, G.G. (2001). Introduction to linear regression analysis. John Wiley and Sons, New York, USA.

Ozdemir, F., Akinci, I. (2004). Physical and nutritional properties of four major commercial Turkish hazelnut varieties. *Journal of Food Engineering*, 63, 341-347.

Saklar, S., Ungan, S., Katnas, S. (1999). Instrumental Crispness and Crunchiness of Roasted Hazelnuts and Correlations with Sensory Assessment. *Journal of Food Science*, 64, 1015-1019.

Torchio, F., Giacosa, S., Río Segade, S., Mattivi, F., Gerbi, V., Rolle, L. (2012). Optimization of a Method Based on the Simultaneous Measurement of Acoustic and Mechanical Properties of Winegrape Seeds for the Determination of the Ripening Stage. *Journal of Agricultural and Food Chemistry*, 60, 9006–9016.

Valentini, N., Rolle, L., Stevigny, C., Zeppa, G. (2006). Mechanical behavior of hazelnuts used for table consumption under compression loading. *Journal of Science of Food and Agriculture*, 86, 1257–1262.

Winton, A.L. (1906). The microscopy of vegetable foods. John Wiley & Sons, New York, USA.

Young, W.J. (1912). A study of nuts with special reference to microscopic identification. US Department of Agriculture - Washington, Govt. Print. Off., USA.

Figure1

Click here to download high resolution image

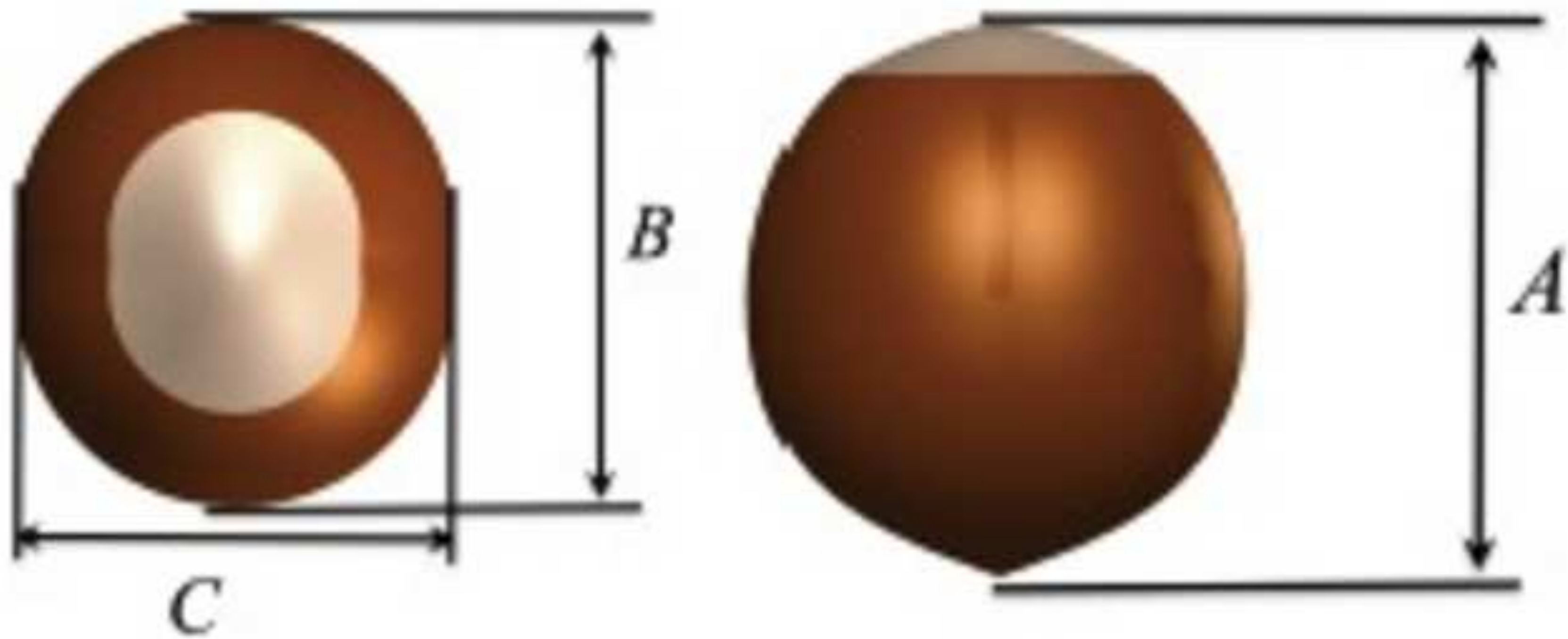

Figure 2
Click here to download high resolution image

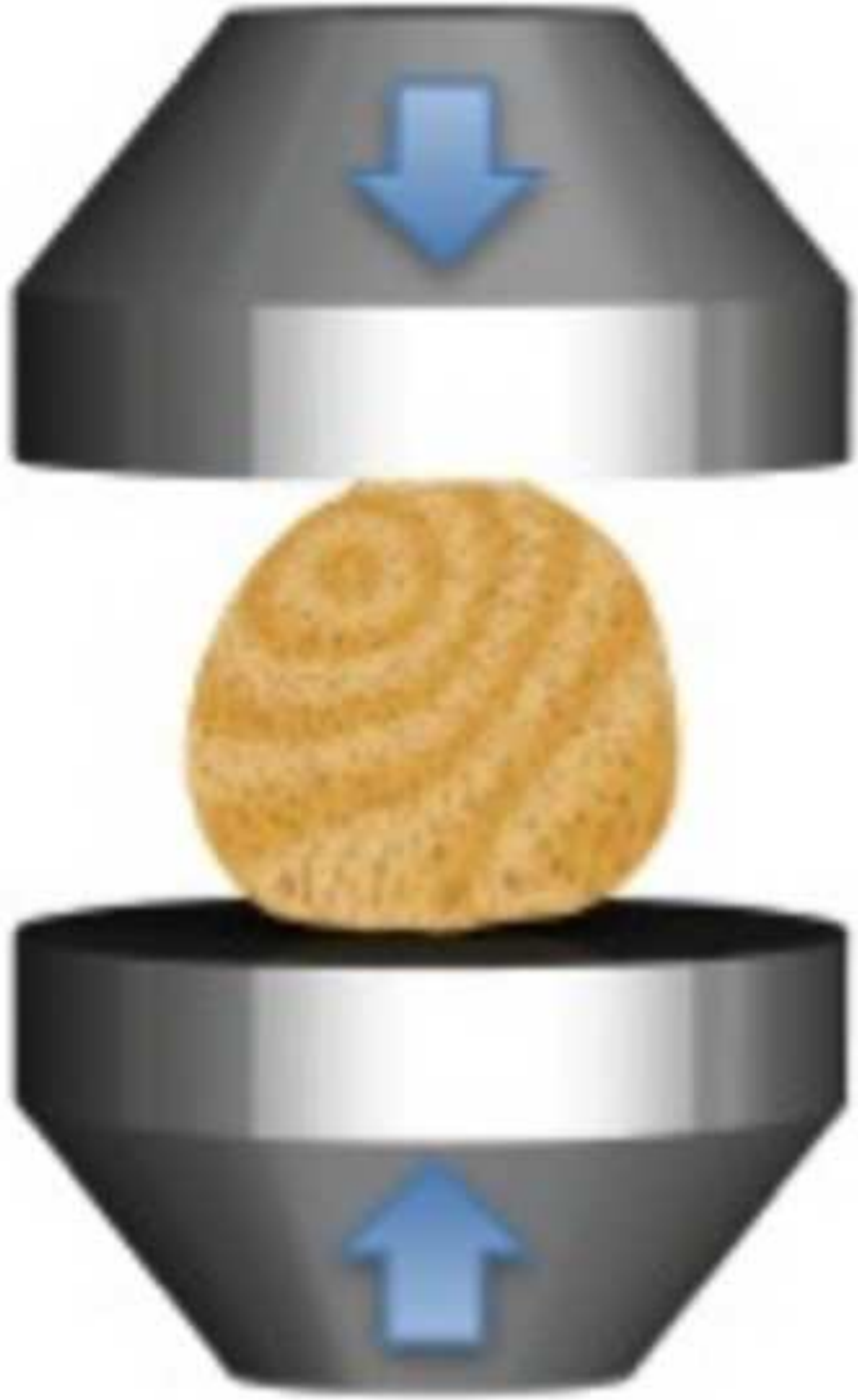

Figure 3
Click here to download high resolution image

Figure 4
Click here to download high resolution image

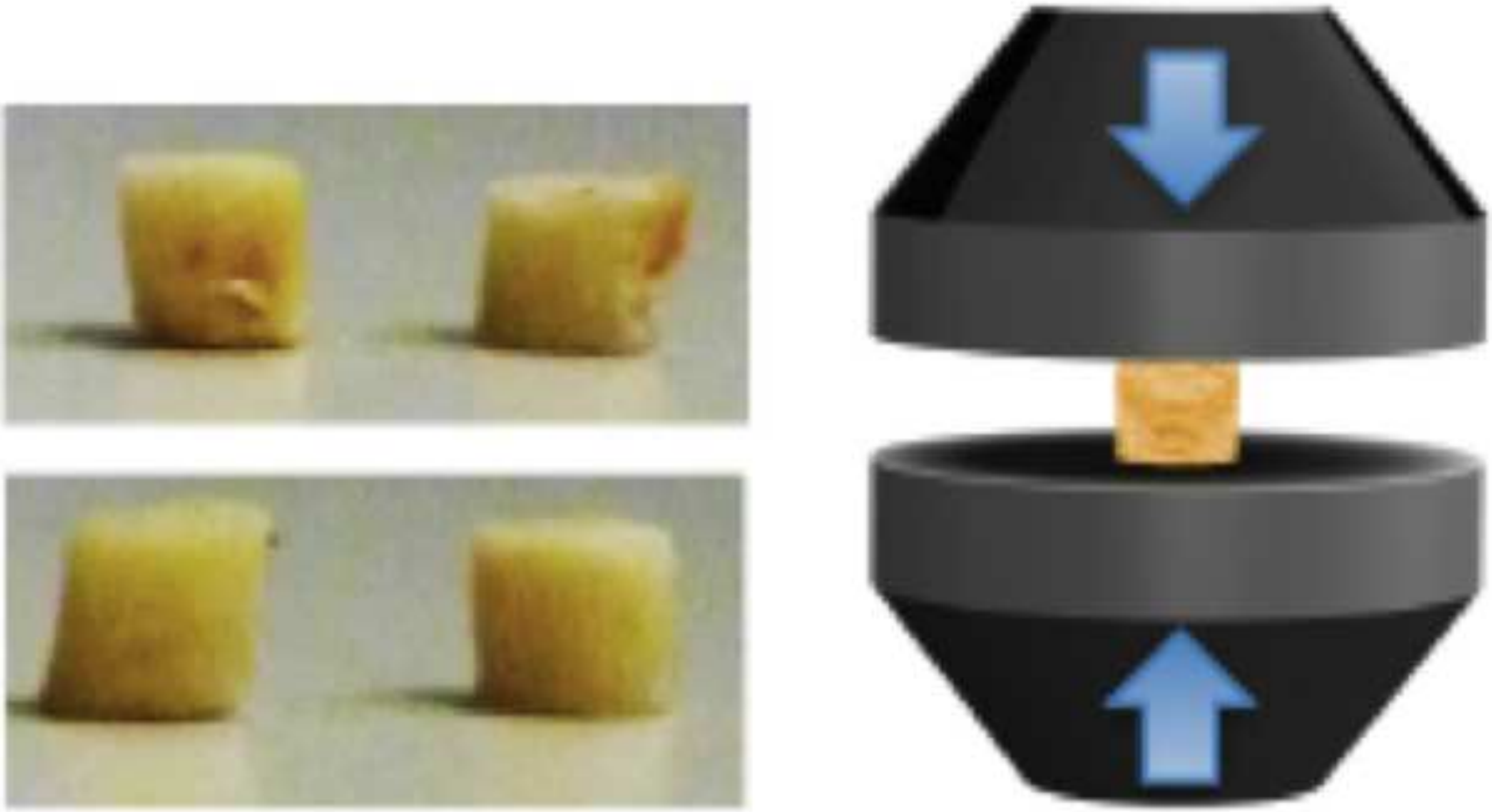

Figure 5
Click here to download high resolution image

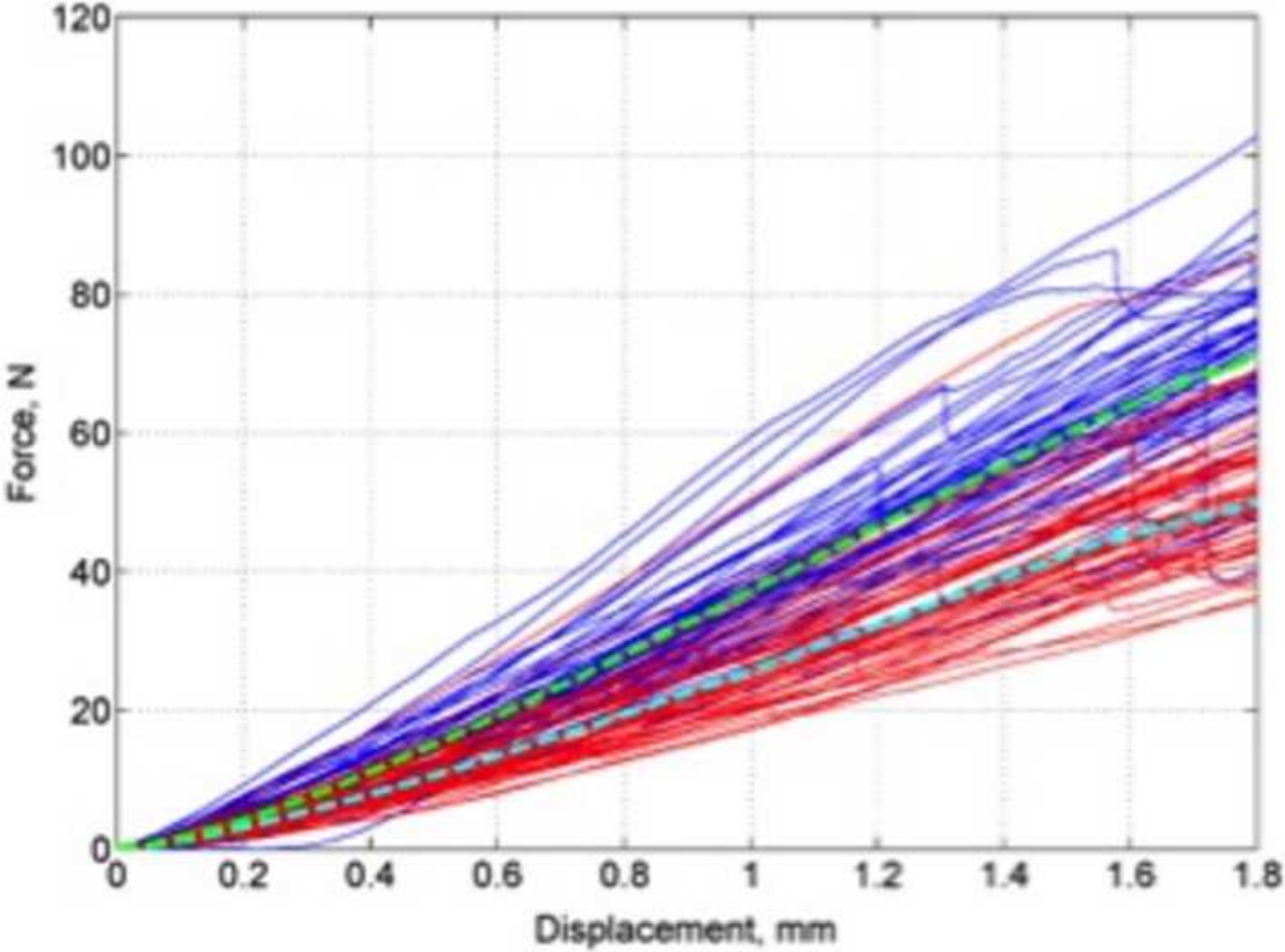

Figure 6
Click here to download high resolution image

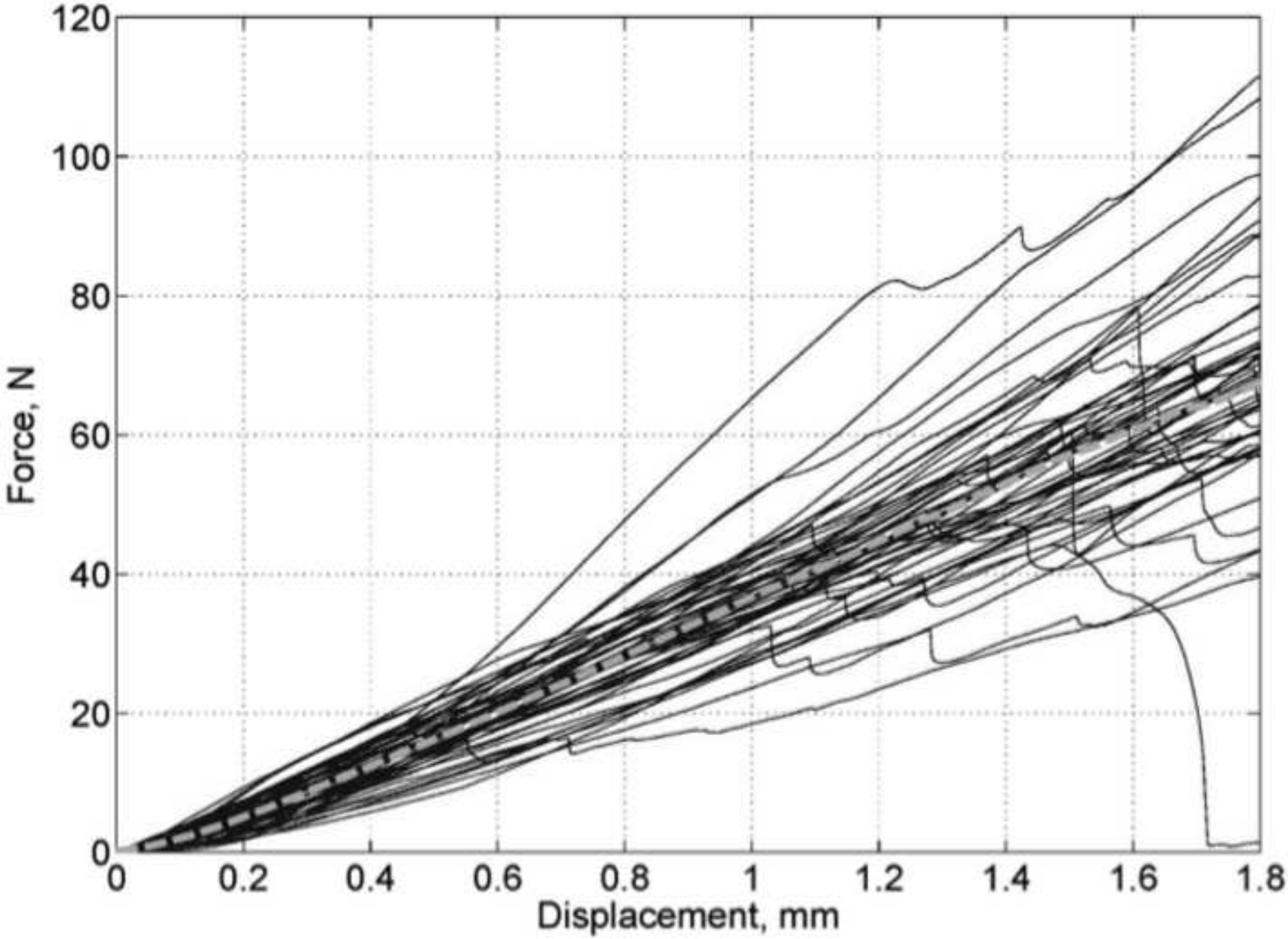

Figure 7
Click here to download high resolution image

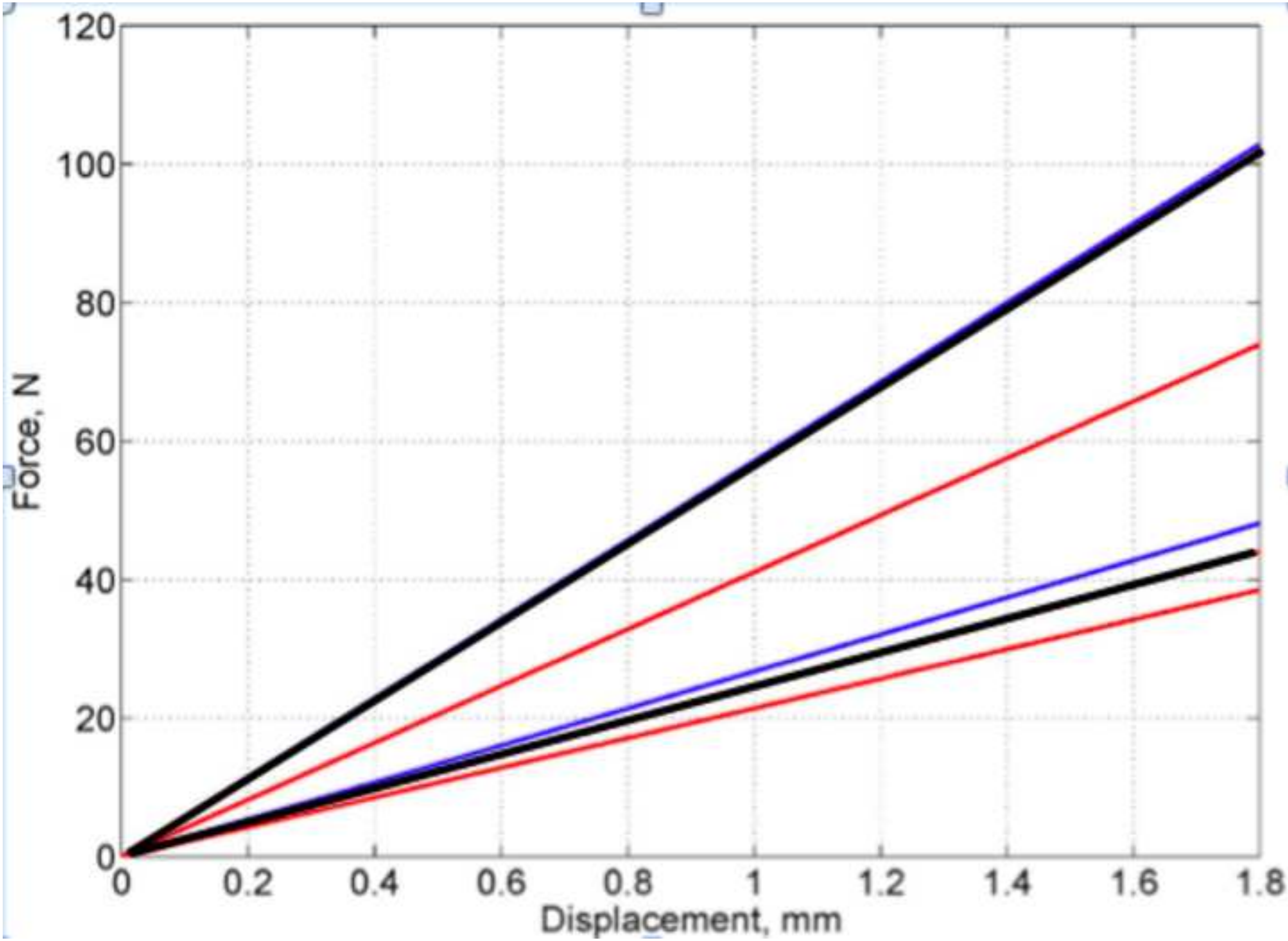

Figure 8

Click here to download high resolution image

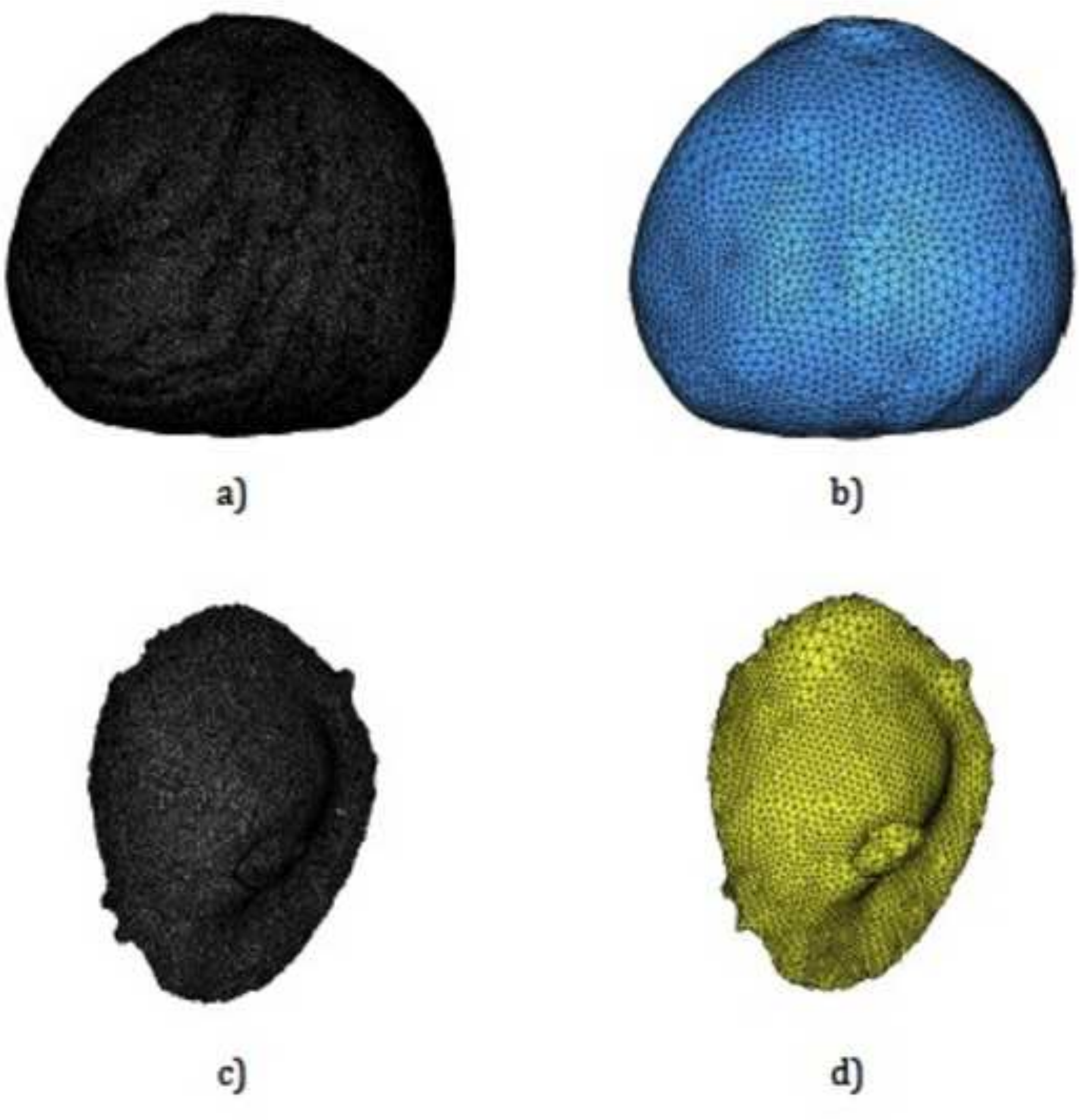

Table 1

Table 1: Elements and nodes of numerical hazelnuts.

CTA number	Nodes	Elements
1	20349	99144
2	15689	76868
3	14768	72014
4	25415	126489

Table 2

Table 2: Average values and standard deviations of physical and geometrical measurements on the specimen samples.

		Average value	Standard deviation	Minimum sample size
Mass [g]		1.27	0.08	43
Geometric parameters	A/B [-]	1.00	0.07	53
	C/B [-]	0.88	0.05	53
	C/A [-]	0.88	0.06	55

Table 3

Table 3: Mechanical properties measurements on the whole kernel samples.

Sample	**Kind of specimens**		**Average value**	**Standard deviation**	**Minimum sample size**	**χ^2 (85% conf. level)**
1	Raw kernels with pellicle	Stiffness $\bar{K}$ [N/mm]	41.93	7.75	42	positive
		$\bar{L}_{kf}$ [N]	83.93	16.33	22	positive
2	Raw kernels without pellicle	Stiffness $\bar{K}$ [N/mm]	31.25	5.02	39	positive
		$\bar{L}_{kf}$ [N]	65.04	16.06	23	positive
3	Toasted kernels without pellicle	Stiffness $\bar{K}$ [N/mm]	40.50	8.19	33	positive
		$\bar{L}_{kf}$ [N]	78.64	29.79	18	positive

Table 4

Table 4: Mechanical properties measurements on the kernel specimen samples.

Sample	**Kind of specimens**		**Average value**	**Standard deviation**	**Minimum sample size**	**χ^2 (85% conf. level)**
4	Raw kernels	Elastic modulus $\bar{E}_k$ [MPa]	11.61	2.68	46	positive
		Stress to failure UCS [MPa]	1.51	0.24	34	positive
		Knee stress σ_k [MPa]	1.23	0.21	27	positive
5	Toasted kernels	Elastic modulus $\bar{E}_k$ [MPa]	10.81	3.43	53	positive
		Stress to failure UCS [MPa]	1.32	0.26	16	positive
		Knee stress σ_k [MPa]	1.12	0.30	41	positive

FIGURES:

Figure 1: Hazelnut shell and kernel main dimensions.

Figure 2: Kernel compression along *A* axis, experimental setup.

Figure 3: Compression failure of hazelnut kernel: cotyledon separation.

Figure 4: Kernel specimens a) and specimens compression setup b).

Figure 5: Force-displacement raw kernel curves with (blue) and without (red) pellicle. Average curves are respectively the green and the cyan ones.

Figure 6: Force-displacement ~~toasted~~ roasted kernel curves with average curve (~~green~~ white).

Figure 6: Raw kernels with (blue continuous lines) and without (red continuous lines) pellicle and ~~toasted~~ roasted without (~~red~~ ~~dotted~~ black continuous lines) pellicle: 95% stiffness values limits.

Figure 7: External a) and internal c) surfaces by CTA and after re-meshing elaboration b) and d).

Figure 8: Comparison between numerical results (black, red and green lines) and 95% limit curves (blue lines).